Hindawi Publishing Corporation
International Journal of Spectroscopy
Volume 2012, Article ID 234949, 14 pages
doi:10.1155/2012/234949

Research Article

On Applicability of a Miniaturised Laser Ablation Time of Flight Mass Spectrometer for Trace Elements Measurements

Marek Tulej, Andreas Riedo, Maria Iakovleva, and Peter Wurz

Space Research & Planetary Sciences, Institute of Physics, University Bern, Sidlerstrasse 5, 3012 Bern, Switzerland

Correspondence should be addressed to Marek Tulej, marek.tulej@space.unibe.ch

Received 13 July 2011; Accepted 19 October 2011

Academic Editor: Michael Balogh

Copyright © 2012 Marek Tulej et al. This is an open access article distributed under the Creative Commons Attribution License, which permits unrestricted use, distribution, and reproduction in any medium, provided the original work is properly cited.

We present results from mass spectrometric analysis of NIST standard materials and meteoritic samples conducted by a miniaturised laser ablation mass spectrometer designed for space research. The mass analyser supports investigation with a mass resolution ($m/\Delta m$) $\approx$ 500–600 and dynamic range within seven decades. Nevertheless, to maintain an optimal spectral quality laser irradiances lower than $\sim$1 GW/cm^2 are applied so far which results in a spread of RSC values. To achieve the quantitative performance of mass analyser, various effects influencing RSC factors have to be investigated. In this paper we investigate influence of laser irradiance, sampling procedure and plasma chemistry on the quantitative elemental and isotopic analysis. The studies indicate necessity for accurate control of laser characteristics and acquisition procedure. A relatively low irradiance applied causes a negligible sample damage and allows for accumulation of large number of waveforms from one sample location. The procedure yields statistically well averaged data and allows a sensitive in-depth analysis. The quantitative analyses of isotopic composition can be performed with accuracy and precision better as 1% and 2%, for isotopic patterns of elements and clusters, respectively. The numerical integration methods would be preferred to achieve more accurate results. The measurements of Allende sample yield detection of Pb isotopic pattern, nevertheless cluster species are readily observed in spectrum and make the elemental analysis of other trace elements difficult due to isobaric interferences. These detections are of a considerable interest because of possible application of the instrument for *in situ* elemental and isotopic analysis and radiometric dating of solids.

1. Introduction

The elemental and isotopic composition of solid materials is a subject of considerable interest to various research fields and a wide range of quite different applications [1]. From the elemental composition, the bulk chemical composition of material can be inferred. Major and minor elements can be used for determination of the material structure and chemistry. Studies of elemental abundances of rocks or soils can provide, for instance, an insight to modal mineralogy [2]. Solid materials contain frequently a low abundant fraction of elements, trace, or ultratrace elements. Investigations of these elements, their distribution in the material, and their temporal abundance changes are subject of gradually increasing interest. Analysis of trace elements can be used for diagnostic of material purity, its heterogeneity, and for process control during manufacturing the high purity materials, for example, semiconductors or special ceramics. By investigation of such processes as corrosion, catalysis, or adhesion effects on the surfaces, the elemental impurities at $\sim$ppm level can play important role in chemical and physical processes [3]. The detection and monitoring of trace elements are used in control of pollution of environmental samples, air, water, plants, animals, and soils that poison agricultural or manufactured products [4]. Studies of isotopes of trace and ultratrace elements (e.g., P, S, Mg, Ca, K, Fe, Cu, Mn) having a vital role in living organisms are of considerable interest and can be used to investigate many biological processes and also the influence of the environment on biological functions [5]. Investigation of trace elements in geological and planetary samples yields unique information on transformation processes on the Earth, planets, and other solar bodies at the scale of the age of our solar system. The element fractionations resulting from

melting and crystallisation of rocks can yield information on planetary differentiation, and isotopic fractionations can be used for a diagnostic of the formation conditions such as volatility-controlled or rare earth element fractionation. Dating of samples and identification of possible biological activities can be derived from the analysis of the details of the isotope variation. Exploration of the surface composition of planets, their moons, and asteroids is planned in most of future planetary missions. Development of instrumentation capable of sensitive and quantitative measurements of elemental and isotopic composition of solid materials is of considerable interest and drives also our present investigations [6].

So far, mostly spectroscopic methods have been used for conducting the chemical analysis of the planetary materials. X-ray fluorescence (XRF) spectroscopy was applied for the detection of elements on the Viking landers on Mars. All Mars rovers to date have also used this technique for conducting the chemical analysis of rocks and soils. This spectroscopic approach yields sufficiently accurate data for determination of the abundances of major and some minor elements. Frequently, however, elements heavier than sodium can be only well determined and the abundance of lighter elements is inferred after extensive background and interelement absorption corrections [7]. The γ-rays and neutron spectroscopic techniques were used for investigation of the elemental abundances of the surface of the Moon, Mars, and asteroids from orbiting spacecraft. These studies brought, for instance, a sensitive detection of potassium and thorium, elements occurring typically in minor and trace abundances. Nevertheless, sensitivity of the element detection by γ-ray and neutron spectrometry depends on counting statistics, and measurement duration in space exceeds months. The spectroscopic instruments have significantly contributed to the analysis of planetary surfaces providing, for example, characterisation of volcanic rocks and sedimentary deposits on Mars or a global database of element abundances on the Moon [8]. Nevertheless, for the measurements of trace elements, analyses of radiogenic isotopes or study of complex organic matter on planetary surfaces and other more sensitive techniques have to be developed. The mass spectrometric approaches are clearly the methods of choice and are preferred because of their higher sensitivity, simplicity of operation, and straightforward data analysis. The time-of-flight mass analysers (TOF MS) are the most convenient in this respect. They can be used to investigate solid materials *in situ* once combined with an appropriate laser ablation ion source.

The mass spectrometric approaches are well established analytical methods in investigation of solid materials. They are most frequently used in laboratory practice for sensitive, accurate, and precise analysis of the elemental composition and determination of trace and ultratrace elements in variety of solid or liquid samples [1]. Developments since 2000 show, however, that the laser-based techniques such as laser ionisation (ablation) mass spectrometry (LIMS) and laser ablation inductively coupled plasma mass spectrometry (LA-ICP-MS) replace systematically other, more expensive approaches and this is in great part due to the progress in development of lasers and fast electronics. LA-ICP-MS is well recognised and frequently used for analysis of ultratrace elements with the detection sensitivities corresponding to sub-ppb g/g. At present stage of the development of this instrument, its application for *in situ* investigation of planetary surfaces is very challenging owing to high complexity of design and operation. Conversely, LIMS or laser ablation mass spectrometry is clearly the method of choice due to its simplicity and robustness.

LIMS uses a laser ablation ion source. Laser radiation is used to ablate untreated samples of any solid material including metals, powders, or glass, and there is no need for special sample preparation procedures (e.g., ovens, chemical agents). The risk of sample loss or its contamination is thus minimised. The ablation process is induced by focusing the laser radiation to a spot of several micrometers allowing investigations of chemical composition with a high spatial (vertical and lateral) resolution and low sample consumption [9–12]. Coupling of laser ablation source with the time of flight mass spectrometer is usually preferred and offers several advantages. The TOF mass spectrometer is highly amenable to pulsed ion sources and its dominant property is fast measurement of transient signals, high sensitivity, and good mass resolution. TOF mass analysers yield a complete mass spectrum for each laser pulse. An ablation/ionisation event generated at each laser pulse is well spatially and temporary localised and initiate clock for counting the time of ion flight from the source to the detector. The mass spectrum is achieved by recording the temporary-resolved signal generated by ion bunches striking an ion detector. The last decade has shown that TOF mass analysers can be miniaturised to 120 mm long cylinder of 50 mm diameter. The weights of the instrument including electronics would be about ~1.5 kg yet maintaining the performance of larger laboratory systems [13, 14]. They can be also operated in extreme environments of temperature, pressure, and radiation. The ROSINA-Rosetta Orbiter Spectrometer is a good example of potential capabilities of a TOF analyser for space research. This reflectron-type time-of-flight mass spectrometer (RTOF) is designed for investigation of charged and neutral gases. It enables studies with mass resolution up to few thousandths, and detection sensitivities better than ~ppm g/g [15]. Further reduction of the size and weight by factor of ~4 could be recently achieved [16]. Several miniaturised TOF mass analysers have been also developed for carrying out the chemical analysis of solids [13, 14, 17] with the LAZMA instrument [18] being part of a payload accepted for missions to Phobos (PHOBOS GROUND) and our Moon (LUNA RESOURCE, LUNA GLOB) [17–20]. These mass analysers are equipped with a laser ablation ion source. This novel approach in space research promises improvements of the elemental analysis *in situ* on solar system body surfaces providing increased elemental sensitivity and complementing results obtained by spectroscopic methods.

LIMS is a sensitive technique, nevertheless, it is still considered to be semiquantitative [11, 21, 22], in spite of its long development history [23]. Complexities introduced by the

ablation process make the quantitative analysis sometimes difficult because of ion yield dependence on laser irradiance, wavelength, pulse duration, or physical properties of the material (morphology, homogeneity). Molecular clusters, frequently accompanying elements in the mass spectra, are formed by plasma chemistry. In addition, a broad and element-specific kinetic energy distribution of ions generated in the ablation process can limit the instrumental mass resolution and cause severe problems for optimal ion detection [24]. In recent developments, control of the plasma process has been partially achieved and advancements in theoretical studies are continued to progress [21]. Achieving the control over the kinetic energy spread of ions generated by ablation is linked with historical development of this technique. Initial success has been achieved by the implementation of a reflectron and other energy focusing devices in the ion-optical system, which resulted in the development of laser-microprobe mass analyser (LAMMA) and later, another versatile system LIMA 2A [25]. The latter system enabled routine qualitative mass spectrometric analysis. Improvements of the design and functionality were also reported after a miniaturisation of laser ablation TOF mass analyser initiated in 1990s by filtering ions of specific energies (energy windowing) [17], or by just applying appropriate ion optics and reflectron combined with ring-shaped detector [13]. Significant improvements of the instrumental performance have been recently achieved by application of novel laboratory LIMS instrument utilising collisional cooling of ions in He buffer gas combined with an orthogonal extraction [26]. The quantitative analysis of the sample composition is, however, not straightforward and requires a careful control of experimental conditions for laser ablation and additional studies of appropriate standard reference materials. The scaling factors have to be achieved for each element and they form the basis for conducting the quantitative elemental analysis of solid samples. Progress in developments and application of laser ablation mass spectrometry in the last decade has been well described in recent comprehensive review articles [21, 22].

Our laboratory develops a miniaturised laser ablation reflectron-type TOF mass spectrometer (LMS) for investigation of chemical composition of surfaces of solar system bodies. Present laboratory efforts are focused on investigation of performance of the instrument. This report extends and follows our recent publication summarising the studies on NIST standard materials, minerals, and meteoritic samples ablated by a nanosecond IR laser radiation [27]. The choice of the IR laser is (although not generally preferred) motivated by simplicity and robustness of this laser. The studies of NIST reference materials, minerals and meteoritic samples have proved high sensitivity of this approach [27]. Nevertheless, low sensitivity in the detection of some nonmetallic elements such as P or S remains and RSCs factors for large number of elements differ clearly from one. To resolve some of possible sources of elemental (isotopic) fractionation, the effects of sampling from one laser spot location, dependence of ion yield on laser irradiance, and formation of clusters are investigated in the present study.

2. Experimental

2.1. Experimental Setup and Principles of Operation. Figure 1 displays a schematic construction of our laser ablation mass analyser. The design and construction details of the mass spectrometer used in the present study can be found in the previous publications [13, 27]. The instrument is located within a UHV chamber that is routinely pumped down to the 10^{-7} mbar range. The sample is placed on X, Y, Z translational stage operated with a position accuracy and resolution in the micrometer range just below the entrance port of the mass analyser. Radiation of a Q-switched Nd:YAG laser system (1064 nm, $\tau \sim 4$ ns, repetition rate 20 Hz) is used to ablate the surface material. The laser radiation is focused to a spot size of about 10 μm at the sample surface by an optical system consisting of beam expander and a doublet lens (f/200, NA = 4). The latter is located just above the reflectron. The laser beam is guided via dielectric mirror system and is aligned colinearly with the ion-optical axis of the TOF mass spectrometer. After entering the mass analyser through the window mounted on the top of the reflectron, it travels along the reflectron and central hole (Ø 6.4 mm) of the detector assembly, ion optical components, all way down until it reaches the sample. The material ablated from the surface forms a hot plasma plume containing atomised and ionised species. Only the fraction of positive ions enters the mass analyser through the conical extraction electrode. After entering to the interior of the analyser, ions are further accelerated, focused, and collimated by an electrostatic immersion lens. Subsequently, ions fly through the field-free region and reflectron where they are reflected towards the multichannel plate (MCP) detector. A pair of multichannel plates arranged in a chevron configuration is used to generate the signal after the ions strike the MCP plate. The ions arrive at the MCP detector in a sequence of times proportional to the square root of their mass-to-charge ratio (m/q). The electron current generated by MCP plates is collected by four concentric anode rings and sent to ADC-card.

The laser system initiates the experimental cycle and triggers the data acquisition. The mass spectra acquired from two different anode rings are fed to two channels of a PCI standard high speed ADC-card (Agilent, U1082A, AP240 with averager firmware). This card supports two channels, each with a sampling rate of 1 GS/s with an analog bandwidth of 1 GHz and vertical resolution of 8 bits for a single shot in a single channel mode. The mass spectra were recorded within a mass range of 0–250 amu/q, which corresponds to the flight times of up to ~20 μs.

Untreated sample pieces of solid material are placed on the sample holder before closing and evacuating the vacuum chamber. The measurements in space could be performed using robotic arm and a rotating wheel sample provider [20]. The sample is positioned at a fixed distance (~3 mm) from the entrance to avoid sample contamination by contact with the outer electrode. The laser fluence was controlled by a polarisation-sensitive attenuator, and the laser irradiances within the range of 0.1–1 GW/cm^2 were applied to ablate the surface. The performance of the mass analyser is limited

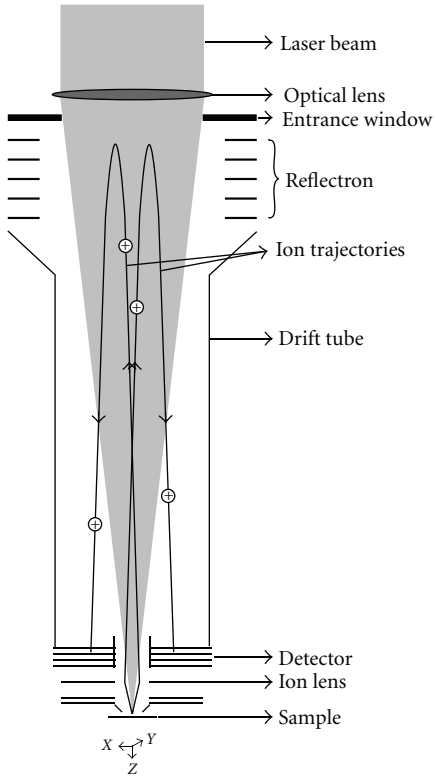

Figure 1: Schematic overview of the laser ablation mass spectrometer used in this study. The instrument is of cylindrical symmetry, 120 mm long and its diameter is 50 mm. The laser beam enters from the top and is focussed on the sample placed on XYZ translational stages at the bottom. Positive ions leaving an ablation plume enter the interior of the analyser through the nose-piece electrode for mass analysis (see text for details).

by charged effects when an excessive amount of ions is generated during ablation process. The space charge effects, such as Coulombic repulsion or sample charging, can cause a deterioration of the instrumental mass resolution.

The mass spectra are measured using signals generated at two of four available anode rings. These are fed into an 8 bit ADC card and accumulated by the averager firmware with up to 64′000 triggers per segment. The averager allows the total vertical resolution of 24 bits corresponding to a maximum of 7 decades of dynamic range per channel. Nevertheless, owing to noise present in the card circuit effective signal to noise of ~4-5 decades per channel can be only achieved and to increase the detection sensitivity two or more channels of different signal gains have to be used. In standard acquisition mode, individual spectra from 64′000 laser shots are added *on line,* for each channel, which are kept at different gain levels. The individual spectra from 1′000 laser shots were acquired in order to control homogeneity of the sample. To maintain linearity, the amplitude range of the high-gain (HG) channel overlaps with the range of the low gain (LG) channel. The effective dynamic range of the detection is increased by factor of about ~140. The LG channel is maintained at the gain at which major elements can be measured at full dynamic range supported by this channel and care is taken to avoid saturation effects. In the HG channel, the minor and trace species can be recorded in with better vertical resolution at an expense of saturation of mass peaks corresponding to major elements.

2.2. Mass Spectrometric Analysis. The TOF mass spectra are measured on a linear time scale t. The transformation into mass scale is made with fixed scaling factors by the relation: $m = c(t - t_0)^2$, where m (amu) is mass t (ns) denotes time of flight and c, t_0 are calibration constants, which are determined experimentally [28]. Because the values of c and t_0 constants depend on the voltage settings of the reflectron and the other ion optical components, they can be subject of minor changes. These constants are obtained as parameters in fitting of the flight times for elements identified in the spectrum. The instrumental mass resolution is typically about $m/\Delta m$ = 500–600. The peak intensities are determined by a direct integration of the peak area with background corrections, which considers the signal baseline next to the individual mass peak. The direct integration is preferred over a curve fitting because asymmetric peak shapes can be observed for some of the intense isotopic components of the major and minor elements. The curve fitting procedure (e.g., Gauss function) would underestimate the abundances of these species. Nevertheless, the exponentially modified Gauss function (EMG) can also be used to model the experimental mass peaks. Signal ringing due to the small impedance mismatch or MCP feedback effects can sometimes be observed for the intense mass peaks along with a periodic high-frequency noise which is collected by ADC card when a large number of waveforms is accumulated. The numerical filtering of these effects can be, if necessary, performed in a straightforward manner.

The mass spectrum resulting from the accumulation of 60′000 waveforms is measured within seven decades of dynamic range for each LG and HG channel. However, three decades are frequently covered by background noise and effective dynamic range of the signal is about four decades for each channel. By combining the LG and HG spectra, an effective dynamic range of 6-7 decades is obtained. The calculations of atomic abundances for major elements are made by integration of the mass peaks from LG spectrum. An independent check from unsaturated mass peaks in the HG spectrum is done by applying the isotopic normalisation procedure. The isotopic normalisation procedure is also used to determine the abundances of elements in case of isobaric interferences and abundances of the trace elements for which only the most intense isotopic components are measured. The performance of the mass analyser is studied using certified NIST standard reference materials (SRM661, SRM664). Because the abundances of elements in the NIST samples are given as weight percentages, w%, they have to be calculated as atomic percentages, a%, for the comparison with our mass spectrometric results. The atomic abundances are subsequently referenced to the most abundant element in the sample. The comparison of the values determined from measurements and abundances quoted by NIST yields the

relative sensitivity coefficients (RSCs), which are a measure of elemental fractionation effects.

3. Results and Discussion

3.1. NIST Standard Reference Materials. The initial measurements of NIST samples (SRM661 and SRM664) have shown high performance of the instrument in terms of mass calibration, mass resolution, and sensitivity [27]. The studies were conducted with laser irradiances (<1 GW/cm^2) somewhat lower than usually applied in laser ablation mass spectrometry (3–8 GW/cm^2) [1]. At these irradiances, relatively slow deepening of the ablation crater and long temporal stability of the ion signal are observed allowing measurement of highly averaged mass spectra from one location. A statistically averaged spectrum, high mass resolution, and measurements of intense and stable ion beam enables preparation of sensitive measurements.

In spite of high sensitivity and reproducibility of the measurements, the quantitative analysis shows that the detection efficiency of different elements can vary significantly.

The correlation between a low detection efficiency and high ionisation potential (IP) could be made for a large fraction of species including nonmetallic elements. Moreover, large RSCs have also been observed, for instance, for Pb and Bi. These could be explained by an enhancement of their concentration in the plasma plume owing to their low boiling temperatures. Furthermore, the detection saturation effects can cause a less sensitive detection of subsequently incoming ions. For example, reduced detection efficiency of Ni, Co elements are observed after detection of Fe ions when studying the NIST SRM661. Figure 2 shows the typical correlation plot between the abundances of the elements quoted by NIST and measured by our instrument. The abundances of metallic elements such as Ti, V, Fe, Mn, and Cr, correlate closely to the quoted values whereas the abundances of nonmetallic elements including C, Si, S, and P can be 100–1000 times lower than the values quoted by NIST.

A number of reasons can contribute to an inaccurate determination of elemental abundances including details of experimental alignment, sampling method, or a poor control over the laser fluence (irradiance). The time-resolved analysis of the ion yield of individual element (isotopic component) and elemental abundances has been performed in parallel with analysis of the evolution of the overall peak envelope. The investigation was conducted by collecting 60 individual spectra at one sample location where each individual spectrum is obtained by adding 1000 waveforms. A sequential analysis of these 60 individual spectra has been performed and the results are displayed in Figure 3. Figure 3(a) shows the temporal variation of the intensity of typical mass peak in the spectrum. An increase of intensity is observed during the first few thousandths of laser shots followed by its abrupt decrease and relatively slow decay until the end of the measurements. Only, small changes of the peak widths are observed and the peak shape evolves from nearly symmetric Gauss-like shape (initially optimised by tuning the voltage settings on the ion optics and reflectron) to the enveloped represented best by the exponentially modified

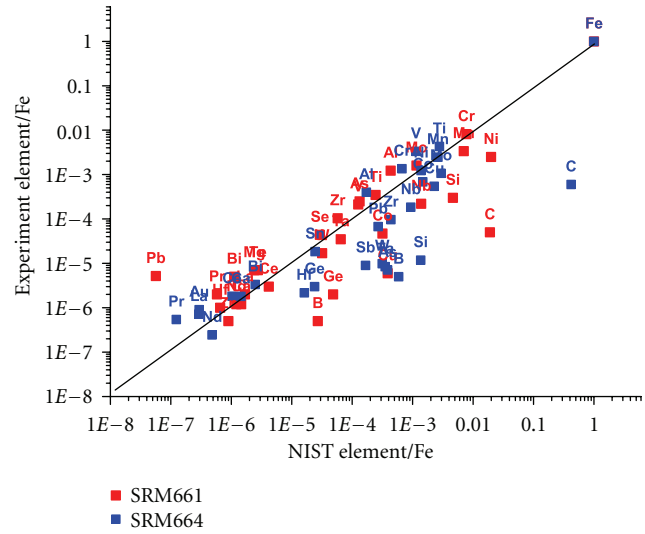

Figure 2: The correlation plot between the elemental abundances of elements quoted by NIST and values determined from the measurements. The measurements underestimate the abundances of nonmetallic elements and elements with high IP's. The abundances of elements possessing low boiling temperatures are, however, clearly overestimated. The measurement of Ni, Co, or Cu abundances suffers from the detector saturation effects caused by saturation detection of ^{54}Fe.

Gauss function with the longer tail directed towards longer flight times. The variations of the peak width and the parameters defining the exponentially-modified Gauss are displayed in the next three panels of Figure 3, respectively. Figure 4 summarises the results from the analysis of the ion yields of individual elements (isotopic components) measured during the initial 15′000 laser shots. First panel to the left displays variation of the elemental ion yield determined after each 1000 laser shots. During the first 5′000 laser pulses, considerable changes of the ion yields for the individual isotopes are observed. The yields of all isotopes are observed to be higher initially and after approximately 5′000 they all drop down but not at the same rates. For some of the elements, the relative yields are observed to reverse with duration of the measurements. This is observed clearly for ^{12}C and ^{98}Mo or ^{48}Ti and ^{51}V. The plot of cumulative sums indicates that the ion yield increases at a different rate for individual elements. The rate of ion yield change tends to stabilise after 10′000–12′000 laser shots. This can be more clearly seen in Figure 4(c) where individual rates of the ion yield change are normalised by the rate of the ion yield of ^{54}Fe.

These results indicate importance of controlling of the measuring procedure for reproducibility of the measurements. Too short measurements would result in the determination of very different elemental abundances than the long ones. A comparable rate of ion yield increase achieved by long sampling procedure guarantees also the reproducibility of the results. Although the elemental abundances measured for NIST standards still differ from the quoted values the determination of RSC factors for the individual elements

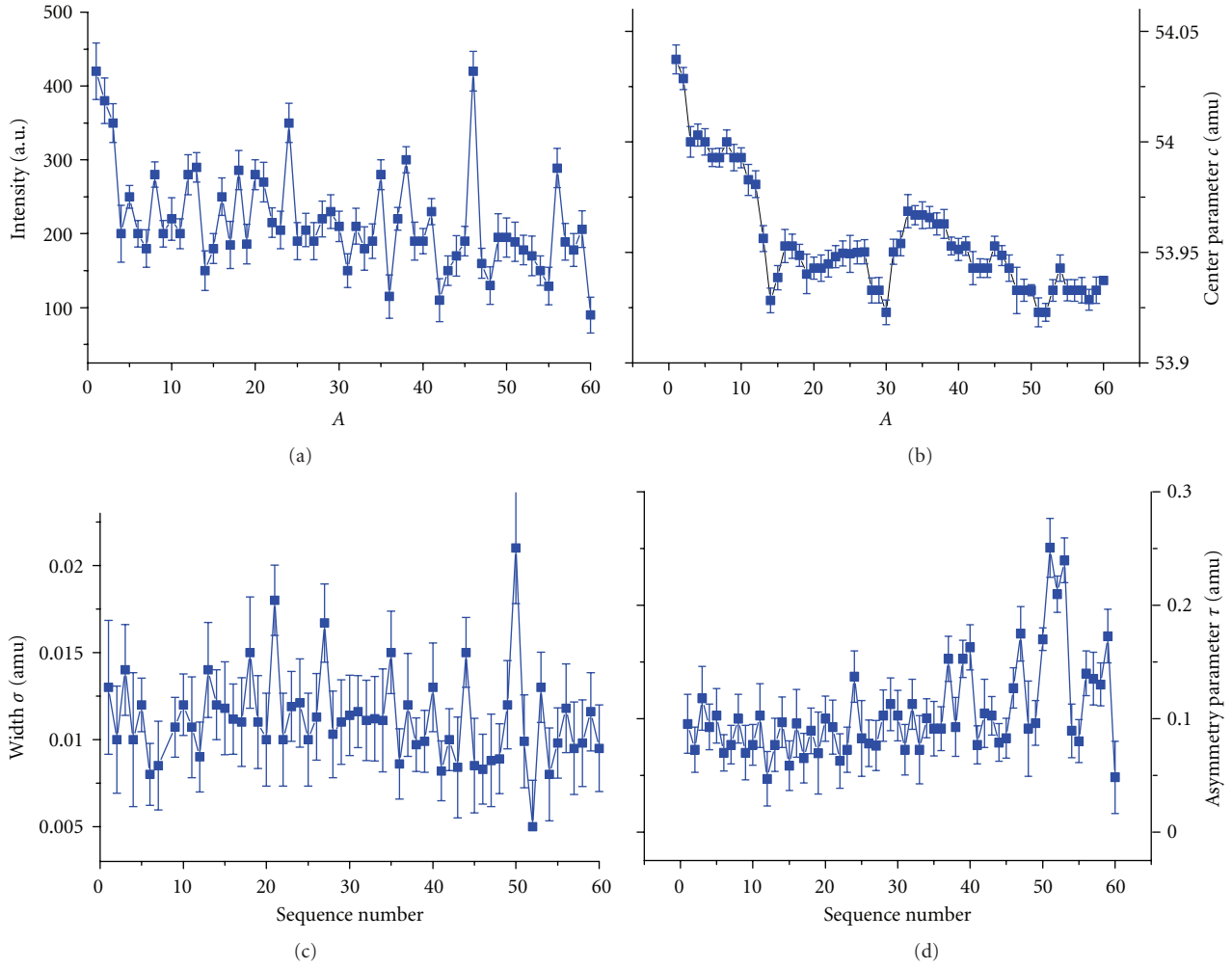

Figure 3: The temporal evolution of the intensity and shape of a typical mass peak during the measurements performed from one sample location. ((a) and (c)) display changes of the peak intensity and its width during the measurements. ((b) and (d)) display temporal changes of the mass peak envelope; the peak centre and exponential decay constant define the exponentially modified Gauss function used to model the experimental mass peak.

can be made on reproducible manner and applied to the quantitative measurements of unknown samples.

Observation of intense spectra during first ~5000 laser pulses can be understood when one assumes that initially the measurements were conducted at higher laser irradiances. Taking into account sharp focus conditions applied in our studies (diameter of laser spot is ~8 μm), a decrease of the peak intensities after 5000 shots may indicate that the ablation front is moving out from the laser focus because of the removal of material from the sample. Due to a deepening of the ablation crater, the effective laser spot diameter interacting with surface becomes larger and, in consequence, laser irradiance decreases. A sharp change of the laser irradiance with number of laser pulses can be expected at ablation conditions where the laser focus is located at the level of the irradiated sample surface. With deepening of the crater, the laser irradiance decrease may cause variation of the ion yield of particular elements (ion yields of particular elements are generally irradiance dependant) and yield time-dependent fractionation of their abundances. Clearly, the measurements performed during this phase can be largely uncertain. The changes of the laser spot size seem to be less dramatic for the rest period of the measurement duration. The observation of a change of the mass resolution and peak shape after this initial phase complements this conclusion. It is well known that at the irradiances used in this study, the ion yield of most elements will depend on laser irradiance [1, 21]. The saturation of the ion yield for most of the elements is observed for irradiances larger than few dozens of GW/cm^2 which corresponds to temperature of the plasma about ~50′000 K [26]. Although sharp changes of the laser irradiance at the sample surface may explain our observation, other effects can also contribute, for example, the appearance of the melting rim. Segregation of the elements during the melting and cooling phases clearly can occur and distort the measurement. In any case, these observations indicate

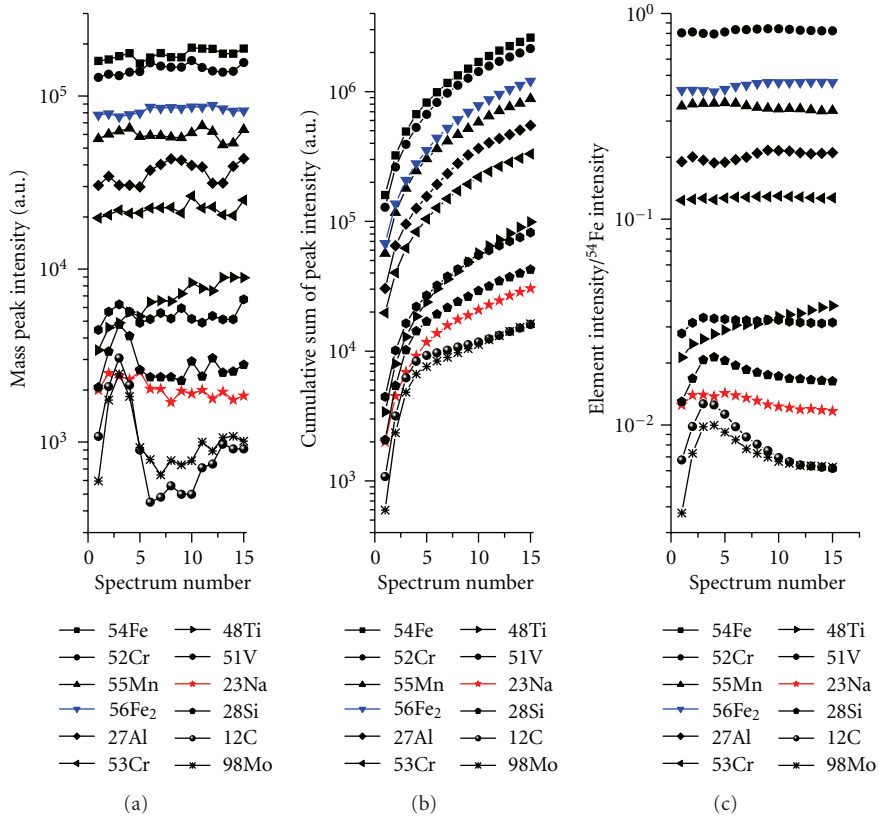

Figure 4: The temporal variation of ion yields of individual isotopic mass peaks recorded after each 1000 laser pulses (a). (b) displays a cumulative sum obtained by accumulation of individual ion yields and reflect the rate of ion yield increase during the measurements. The cumulative sums of the ion yields of the individual isotopic components of elements and clusters normalised to the cumulative sum of the ion yield of ^{54}Fe are displayed in (c).

that due to large changes in ion yield observed during the initial few thousandths of laser shots may introduce errors in the abundance determination. It seems, however, that these effects are become well averaged after 15′000 laser pulses. Nevertheless, too long laser sampling from one location may exert material changes due to long-term melting and recrystallisation (melting rims). These can result in changes of the material properties or possible sample damage. Apart to the control of sampling duration, the control over the sample position against the laser focus and laser fluency is essential for achieving quantitative and reproducible results.

Figure 5 displays part of two mass spectra of the NIST SRM661 reference sample obtained in the mass region where B, C, P, and S should be detected. The mass spectra are recorded at irradiances of ~0.3 and ~1 GW/cm^2, respectively. An enhancement of the intensity of the mass peaks of B and C can be observed comparing the low and high irradiance spectra. Isotopic components of ^{10}B, ^{11}B, ^{12}C, and ^{13}C can be seen as well demonstrating a large dynamic range in these spectra. The abundance of the element B in SRM661 quoted by NIST is 5 ppm, corresponding to ^{10}B and ^{11}B isotope abundances of 1 and 4 ppm, respectively. The abundance of C is 0.39% by weight, corresponding to ^{12}C and ^{13}C isotopic abundances of 3900 and 42 ppm, respectively. The isotopic ratios for ^{10}B and ^{11}B isotope determined from the spectra are 21.0% and 79.0%, respectively, compared to the tabulated values of 19.9% and 80.1%. For ^{12}C, and ^{13}C these values are 99.27% and 0.73%, respectively, compared to the tabulated values of 98.9% and 1.07%.

The RSC factors for B and C elements determined from the spectrum in lower panel are of the order of ~0.01 and ~0.001, respectively. These factors are about one order of magnitude larger when the higher irradiance is applied. Other trends of ion yield dependence is observed in a previous report [29]. With increase of the laser fluence, lower abundances of atomic ions were observed but an increase in abundance molecular species composed from these elements.

The RSC factors for S and P are similar to that of C (a rough estimation of RSC factor for S from the studies of Galena sample yields RSC~0.001 at ~0.3 GW/cm^2 [27]). The S and P elements have not been detected in our previous measurements of the NIST samples due to their low abundances (~150 ppm) and low RSC. At higher laser irradiances applied in the present study, a small mass peak of ^{32}S can be measured on the extensively perturbed background curve caused by the saturation detection of Al peak. These studies indicate that the RSCs for the nonmetallic elements can be still improved by applying higher laser irradiances. Unfortunately, at present stage of

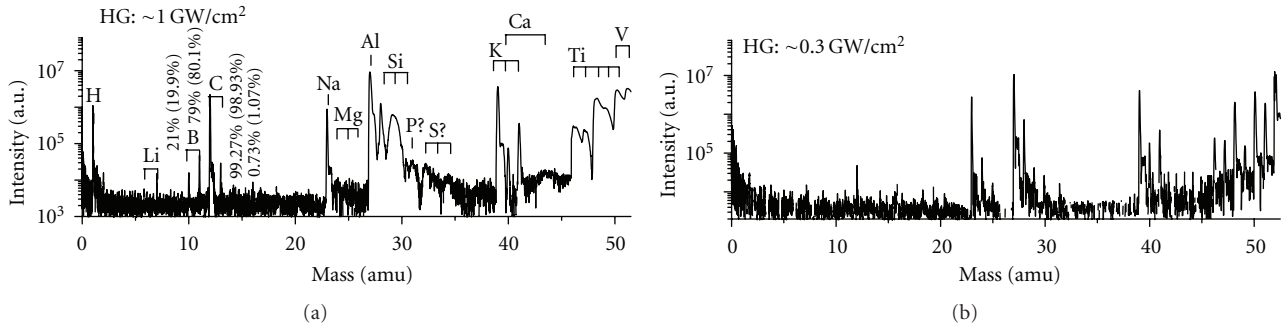

Figure 5: Part of two mass spectra obtained at different laser irradiances. The spectrum in (a) shows an increase of the detection efficiency for C and B elements. The mass peak broadening observed in (a) is attributed to space charge effects resulting from the increased ion abundances.

the instrument development, an increase of laser fluence can cause a large decrease of spectral quality. Broadening of the most intense mass lines of the major and minor elements (see Ti, V mass peaks in the upper panel) is clearly observed. Notice that the mass peaks corresponding to low abundant species are still considerable narrow. The broadening is likely caused by space-charge effects (Coulombic repulsion) and could not be compensated by focussing capabilities of the reflectron. The threshold of the ion yield saturation for most of elements is expected for irradiances an order of magnitude larger than applied in an present investigations ($\sim$10 GW/cm^2) [30]. The ion yield of most of elements is observed to saturate for most of materials by applying even higher irradiances [21]. Existence of threshold energy is in accordance to several experimental and theoretical studies. In case of metallic samples, the energy threshold depends on the cohesive energy of the metall [31].

Thermal processes induced during ablation of the material by nanosecond lasers cause vaporisation, atomisation, and ionisation of the elements owing to high plasma temperature. However, during the expansion of the plasma plume cooling, recombination processes begin to play a role and molecular fraction can be built up. At relatively low laser irradiances $\ll$0.1 GW/cm^2 molecules or clusters residing on the surface of a solid material can be also removed via desorption into gas phase. Recently, our instrument has been, for instance, used to measure a fraction of carbonaceous contamination on charge state conversion surfaces [32]. In the present investigations, the mass spectra of SRM664 sample have been recorded at quasidesorption (about 10 MW/cm^2) and ablation ($\sim$0.4 GW/cm^2) conditions (Figure 6). The spectra were taken in LG channel, each time from a fresh surface location. Intense mass peaks of metallic oxides (MeO_x), clusters, and cluster oxides were measured. The application of higher laser irradiance removes rapidly the oxidation layer, and the characteristic isotopic pattern of low abundant Fe_2 cluster can be only seen. Other metallic clusters and sometimes residual abundances of iron oxides can also be observed in the spectra recorded in HG channel ($\sim$100 times amplified signal). These clusters can be built up via plasma chemistry. The cluster abundances do not change significantly with an increase of the laser fluence. Only for irradiances close to $\sim$10 GW/cm^2, a considerable reduction of cluster contribution was observed [33]. Nevertheless, even for much higher irradiances, clusters are not disappearing and can cause isobaric interferences [29]. Due to deficiency of oxygen in the SRM standards, the molecular fraction containing various oxides is reduced providing basis for the analysis of elements in the mass range of 63–160 amu. Noticeable is also a decrease of abundances of Na and K. These elements are not present in the NIST sample but frequently are observed as a contamination of sample surface.

The relative abundances of oxides and clusters observed in our studies are qualitatively consistent with previous reports. By using IR laser, a thermal ablation mechanism is appropriate for the description of ablation process, which explains formation of clusters and reduced abundances of oxides. The laser fluence change may exert competitive effects on cluster formation. Increase of the laser fluence can cause an increase of the plasma densities and the rate of cluster formation. On the other hand, the plasma temperature increase can result in a destabilisation of clusters or even disable larger cluster formation [34]. For low laser irradiances ($<10^7$ W/cm^2), the clusters can be formed via desorption/ionisation mechanism, but at larger irradiances, plasma chemistry is essential [35, 36]. When UV radiation will be used for ablation, further reduction of cluster abundances is to be expected owing to an enhancement of the rate of photodissociation processes induced by more energetic UV photons [37]. A complete absence of clusters is observed when a short pulse duration laser beams are applied [38].

The assignment of the mass peaks in the spectra of SRM661 and SRM664 is straightforward for masses smaller than 63 amu. For mass peaks of heavier elements, one has to consider possible interferences caused by presence of clusters and oxides. To assess the contribution of clusters in the spectrum, a good isotopic signature of the cluster mass peaks is necessary. Previous studies show a good performance of the instrument for investigation of the isotope ratios of elements [27]. The isotopic ratios could be determined with

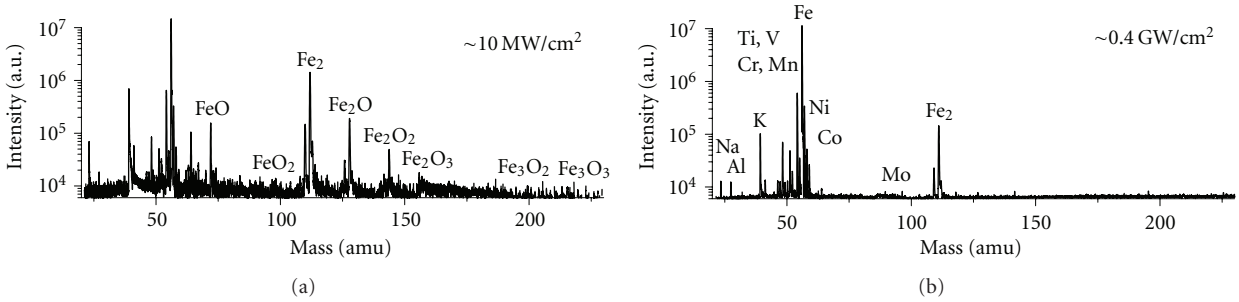

Figure 6: The mass spectrum of SRM664 sample recorded in quasidesorption (a) and ablation mode (b). Both, elements and clusters can be measured and assigned considering their isotopic pattern.

the uncertainty better than 1%. This knowledge can be used for determination of elemental abundances in case of isobaric interferences caused by an overlap with other elements or clusters by taking into account the standard isotopic normalization procedure. However, the detection of trace elements, for which sometimes only the most intense isotopic components can be observed, has to be considered with a care owing to multiplicity of possible isotopic components of clusters (see, e.g., next sub-section). Figure 7 shows the mass spectra of Fe, Mo, and Pb, their oxides/sulphides, and clusters. The measurements of Fe species were conducted on NIST SRM664 sample (in quasidesorption mode), studies of Mo species-on high purity Mo material, and Pb clusters were measured using Galena sample. In case of Fe species, a small contamination due to abundances of other minor metallic elements may interfere with the Fe isotopic lines and isotopic Pb ratios are affected by a fine natural fractionation, respectively.

Table 1 shows the calculated and measured isotopic abundances of element, oxide/sulphide, and clusters. The abundance ratios of isotopic components for cluster, oxides, or sulphides are obtained using their natural abundance ratios. The relative abundances of diatomic clusters are calculated using multi-nominal expansions, which are well-known expressions [39]. The isotopic abundances are normalised to 100%, their values are given in Table 1. Usually they do not differ by more than 2% of the values calculated from the appropriate expressions. The calculated isotopic percentages are compared with measured ones and represented as bar spectra in Figure 7. The errors of isotopic fractions of oxides/sulphides and clusters are somewhat larger than those for elements, which may be partially attributed to accuracy of the integration method and possible fractionation caused by plasma chemistry. In principle, the mass peaks corresponding to elements could be extracted from the spectra contaminated by diatomic clusters by subtracting cluster isotopic pattern modelled from the terrestrial isotopic composition of corresponding element. One has to be aware, however, that the fractionation effects due to chemical recombination reactions in plasma may be large and are species- and cluster-specific. Fractionation effects caused by chemistry can be clearly observed in the relative abundance distribution of various oxides and clusters. They do not follow strictly the elemental abundance distribution. The knowledge of the isotopic distribution of clusters can be helpful for conducting the quantitative control and is of considerable interest in speciation analysis [36].

3.2. Allende Sample. In our previous study, the applicability of the instrument to study of planetary samples has been demonstrated by measurements of the elemental composition of the sample of Allende meteorite [27]. Light elements (Li, Na, Mg, Al, K, Ca) and heavier elements (Ti, V, Cr, Mn, Fe, Ni, Co) could be measured. With a careful control of the experimental conditions and calibration of elemental abundances by appropriate standard, the diagnostic of meteoritic material and its assignment to appropriate meteoritic class can be made [27]. Allende belongs to the group of carbonaceous chondrites (CV3) having primitive chemical composition, meaning that its composition changed only slightly from the time of their formation [40]. The studies of trace elements distributions in highly heterogeneous structure of the Allende meteorite (chondrules, calcium aluminium-rich inclusions (CAIs), fine-grained regions, and several mineral phases) are of considerable interest. They can allow inferring the roles of various types of elemental fractionations in the solar system, including sorting and segregation of chondrite components. Our investigations of standard materials show clearly possibilities for detection of elements abundant at sub-ppm and have stimulated present investigations.

Figure 8 displays a typical mass spectrum of Allende sample. The spectrum can be measured within 6-7 decades of the effective dynamic range, and the analysis of element abundances can be made with the support of the experimental RSC factors for almost all elements up to 63 amu [27]. Nevertheless, the assignment of heavier elements can be difficult due to presence of abundant metallic oxides and clusters. These can be identified in the spectrum taking into account their characteristic isotopic patterns and the mass peaks of iron species clearly dominate in the spectrum (see Figure 9). Although assignment of most of mass peaks can be made relatively easy studying isotopic patterns of metallic clusters and their oxides the contribution of the elements could not be safely elucidated due to spectral complexity. Thus, with the exception of Pb, the identification of other elements could not be made safely this time.

Table 1: Measured and calculated isotope abundance ratio of Fe, Mo, and Pb oxides/sulphides and their diatomic clusters determined from the experiment and calculated from the multi-nominal expansions. The values marked by (∗) are adopted from the calculation.

Element /cluster	Exp. abundance %	Nat. abundance %	Element /cluster	Exp. abundance %	Nat. abundance %
Fe			Pb		
54	5.834	5.845	204	1.5	1.4
56	91.773	91.754	206	24.6	24.1
57	2.111	2.119	207	21.6	22.1
58	0.282*	0.282	208	52.4	52.4
FeO			PbS		
70	5.45	6.12	236	1.419	1.331
71	0.32	0.48	237	0.010*	0.010
72	88.22	88.93	238	24.415	22.972
73	5.70	2.56	239	21.768	21.192
74	0.93	0.94	240	52.273	50.923
75	0.49*	0.49	241	1.334*	1.334
76	0.48*	0.48	242	2.9	2.231
			244	0.002*	0.002
			245	0.005*	0.005
Fe_2			Pb_2		
108	0.66	0.40	408	0.018*	0.018
110	10.30	10.73	410	0.63*	0.63
111	0.41	0.31	411	0.57*	0.57
112	82.95	83.86	412	5.607	6.75
113	4.71	3.93	413	9.479	9.89
114	0.97	0.62	414	29.00	35.16
115	0.07*	0.07	415	19.456	21.50
116	0.06*	0.06	418	36.457	25.48
Mo			Mo_2		
92	14.78	14.77	184	1.945	2.079
94	8.66	9.23	186	2.234	2.598
95	16.32	15.90	187	4.293	4.476
96	18.02	16.68	188	5.415	5.508
97	9.61	9.56	189	5.396	5.489
98	23.41	24.19	190	11.72	12.15
100	9.20	9.67	191	7.27	6.74
			192	12.23	17.22
			193	11.33	10.37
			194	10.55	10.26
			195	8.18	7.34
			196	9.89	8.65
			197	1.64	1.76
			198	6.56	4.46
			200	1.34	0.89
MoO					
108	14.40	14.734	114	25.47	24.169
109	0.006*	0.006	115	0.029*	0.029
110	8.90	9.238	116	9.810	9.696
111	15.90	15.865	117	0.004*	0.004
112	16.60	16.664	118	0.020*	0.020
113	9.30	9.576			

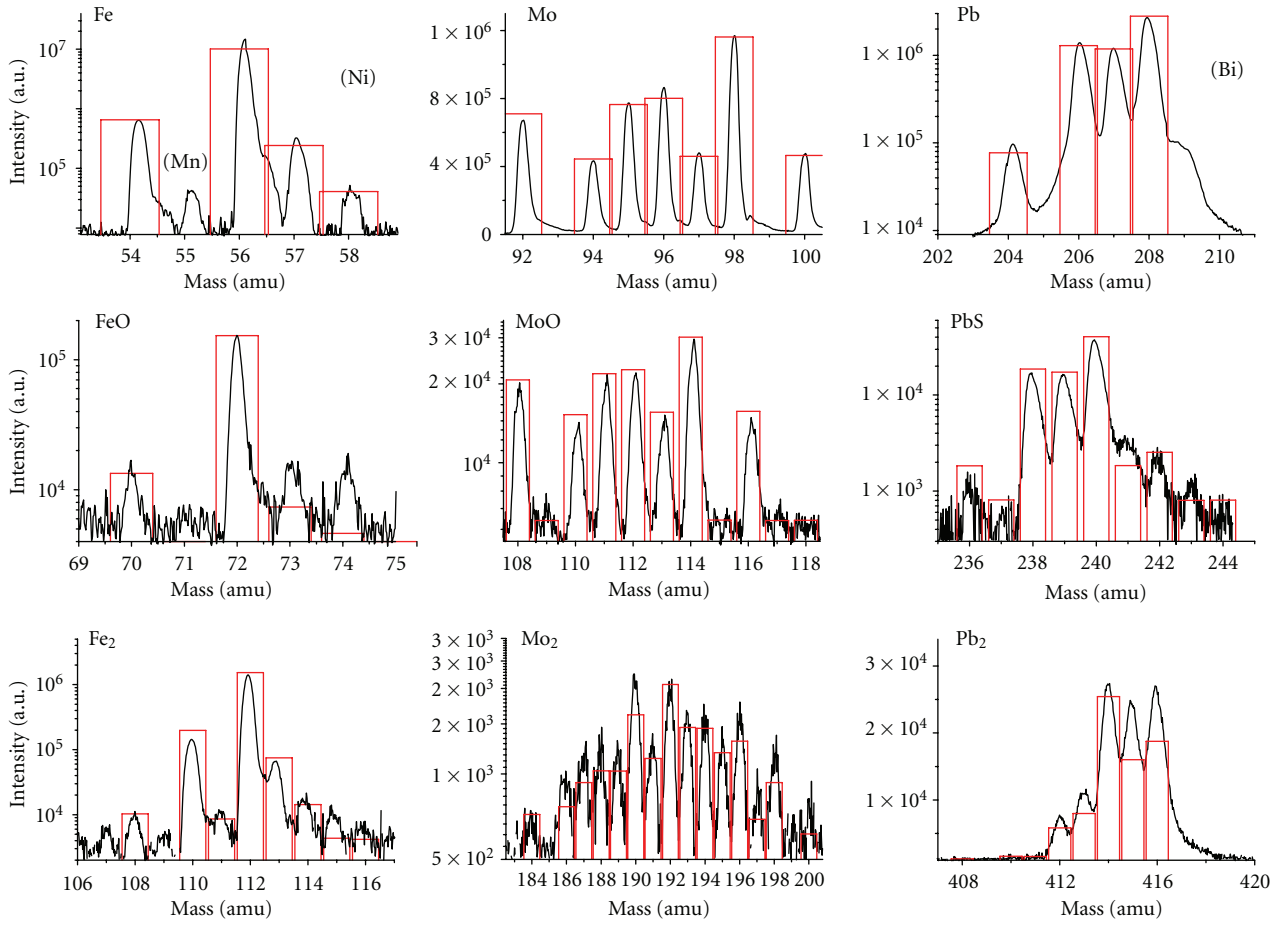

Figure 7: Isotopic pattern of Fe, Mo, and Pb elements and their oxides and clusters. Bar spectra of oxides and clusters represent isotopic pattern calculated from natural isotopic distribution of accompanying elements. The isotopic abundances of elements are usually reproduced with 1% accuracy whereas the isotopomers of oxides and clusters can be measured generally within 2% of the calculated value.

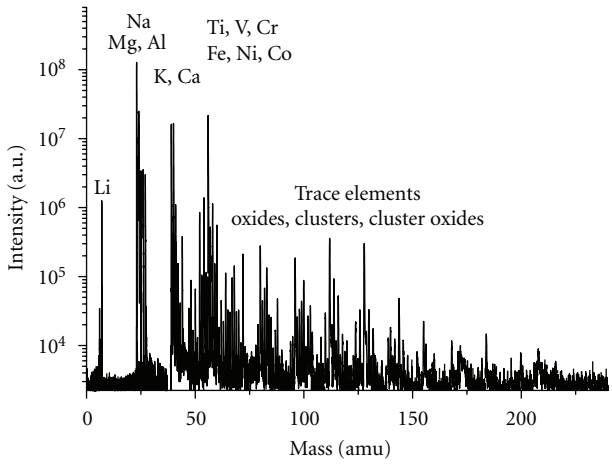

Figure 8: A typical mass spectrum of Allende sample, which can be measured at various sample locations. Similar mass peak distributions, relatively insensitive to laser irradiance increase are observed in the mass range corresponding to trace elements and are attributed to metallic oxides, clusters, and cluster oxides.

The observation of abundant metallic clusters and oxides in the studied meteoritic sample is not surprising. Owing to high affinity of metallic elements to oxygen, their oxides can be formed relatively easy due to plasma chemistry. In contrast to NIST standard materials, where oxygen content in the sample is very low, the detection of trace elements can be made with a high confidence whereas the detection of trace elements in mineral samples can be more difficult due to isobaric interferences caused by presence of clusters. Abundances of oxides detected in present study could not be reduced by applying higher laser irradiances. Other laser ablation studies show as well that the formation of clusters and oxides is not avoidable and results from variety of chemical processes which can take place in plasma [41–45].

The trace element analysis by laser ablation mass spectrometry can be sometimes difficult for complex mineral samples and isobaric interferences due to presence of oxides and clusters can limit detection efficiency. An ablation process induced by ns-lasers is complex owing to several competing processes and rich plasma chemistry. Nevertheless, ablation studies by lasers with pulse durations in

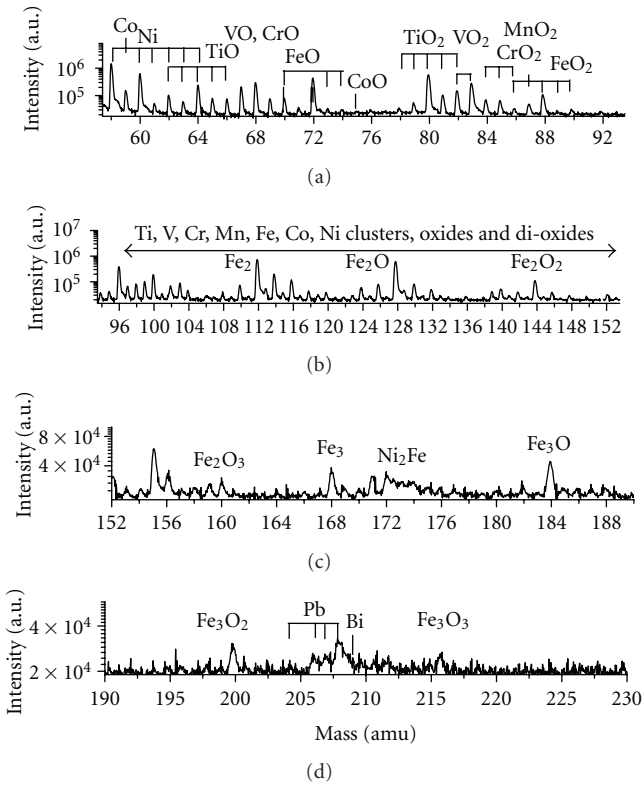

Figure 9: The assignment of the mass spectrum recorded in the mass range corresponding to heavier trace elements. Appearance of the most mass peaks is consistent with the observation of clusters and their oxides, which can be confirmed considering their characteristic isotopic patterns.

picosecond or femtosecond range are expected to improve the performance of our analyser. A femtosecond-laser-induced ablation process can result in a significant reduction or even absence of interfering clusters and oxide.

4. Summary

A miniaturised laser ablation time of flight mass spectrometer designed for planetary research has been used to study the elemental and isotopic composition of untreated solid samples. The instrument is capable of recording well-calibrated mass spectra and its mass resolution can be higher than ~600. A high sensitivity of the measurements could be achieved in studies of NIST standard samples and the detection of trace elements at a sub-ppm level could be performed. For reproducibility of the measurements, however, well-defined measuring procedure has to be maintained. Present studies investigate influence of the sampling duration and the laser irradiance on reproducibility of the measurements. Appropriate control over the number of laser pulses used for the ablation is essential for reproducibility of the results and determination of relative sensitivity factors in studies of standard reference materials. These can be subsequently used for the quantitative measurement of elemental composition of unknown samples. However, for complex samples containing several metallic elements and abundant in oxygen/sulphur, severe contamination in mass range 63–200 is to be expected due to formation of oxides and clusters. These can make sometimes studies of heavier trace elements difficult due to isobaric interferences.

The isotopic abundance ratio can be measured typically within 1% of the value given from the standard isotopic distribution. The abundances of isotopomers of clusters can be measured within 2% of the value calculated from multinominal expansions indicating a good quantitative performance of the instrument for conducting the isotopic measurements.

Present study provides hints for the improvements of the quantitative capabilities of the instrument. The control over the experimental conditions such sample alignment and standard instrumental performance in terms of mass resolution is essential. Nevertheless, one of the main reason for a semiquantitative performance of the instrument seems to be the application of ns-resolved infrared laser radiation for the ablation of sample. The elemental fractionation effects in the detection of nonmetallic elements are relatively large and readable abundances of clusters and oxides formed via plasma chemistry are observed. The activities aimed at a more precise control over the laser fluence/irradiance, better accommodation of the plasma plume at higher irradiances are now undertaken along with application of other laser systems including also short-pulse duration lasers.

Acknowledgments

Technical support from Harald Mischler is gratefully acknowledged. This work is supported by the Swiss National Science Foundation.

References

[1] J. S. Becker, *Inorganic Mass Spectrometry*, John Wiley & Sons, 2007.

[2] K. E. Jarvis and J. G. Williams, "Laser ablation inductively coupled plasma mass spectrometry (LA-ICP-MS): a rapid technique for the direct, quantitative determination of major, trace and rare-earth elements in geological samples," *Chemical Geology*, vol. 106, no. 3-4, pp. 251–262, 1993.

[3] V. Hoffmann, M. Kasik, P. K. Robinson, and C. Venzago, "Glow discharge mass spectrometry," *Analytical and Bioanalytical Chemistry*, vol. 381, no. 1, pp. 173–188, 2005.

[4] C. J. Koester and A. Moulik, "Trends in environmental analysis," *Analytical Chemistry*, vol. 77, no. 12, pp. 3737–3754, 2005.

[5] R. Lobinski, C. Moulin, and R. Ortega, "Imaging and speciation of trace elements in biological environment," *Biochimie*, vol. 88, no. 11, pp. 1591–1604, 2006.

[6] P. Wurz, D. Abplanalp, M. Tulej et al., "In situ mass spectrometric analysis in planetary science," *Solar System Research*. In press.

[7] R. Rieder, T. Economou, H. Wänke et al., "The chemical composition of martian soil and rocks returned by the mobile alpha proton x-ray spectrometer: preliminary results from the x-ray mode," *Science*, vol. 278, no. 5344, pp. 1771–1774, 1997.

[8] H. Y. McSween Jr., R. L. McNutt Jr., and T. H. Prettyman, "Spacecraft instrument technology and cosmochemistry," *The Proceedings of the National Academy of Sciences of the United States of America*, pp. 1–6, 2011.

[9] L. A. McDonnell and R. M.A. Heeren, "Imaging mass spectrometry," *Mass Spectrometry Reviews*, vol. 26, no. 4, pp. 606–643, 2007.

[10] R. Huang, B. Zhang, D. Zou, W. Hang, J. He, and B. Huang, "Elemental imaging via laser ionization orthogonal time-of-flight mass spectrometry," *Analytical Chemistry*, vol. 83, no. 3, pp. 1102–1107, 2011.

[11] J. S. Becker and H. J. Dietze, "State-of-the-art in inorganic mass spectrometry for analysis of high-purity materials," *International Journal of Mass Spectrometry*, vol. 228, no. 2-3, pp. 127–150, 2003.

[12] L. Matus, H. M. Seufert, and K. P. Jochum, "Microanalysis of geological samples by laser plasma ionization mass spectrometry (LIMS)," *Fresenius' Journal of Analytical Chemistry*, vol. 350, no. 4-5, pp. 330–337, 1994.

[13] U. Rohner, J. A. Whitby, and P. Wurz, "A miniature laser ablation time-of-flight mass spectrometer for in situ planetary exploration," *Measurement Science and Technology*, vol. 14, no. 12, pp. 2159–2164, 2003.

[14] U. Rohner, J. A. Whitby, P. Wurz, and S. Barabash, "Highly miniaturized laser ablation time-of-flight mass spectrometer for a planetary rover," *Review of Scientific Instruments*, vol. 75, no. 5, pp. 1314–1322, 2004.

[15] H. Balsiger, K. Altwegg, P. Bochsler et al., "Rosina—Rosetta orbiter spectrometer for ion and neutral analysis," *Space Science Reviews*, vol. 128, no. 1–4, pp. 745–801, 2007.

[16] D. Abplanalp, P. Wurz, L. Huber et al., "A neutral gas mass spectrometer to measure the chemical composition of the stratosphere," *Advances in Space Research*, vol. 44, no. 7, pp. 870–878, 2009.

[17] W. B. Brinckerhoff, G. G. Managadze, R. W. McEntire, A. F. Cheng, and W. J. Green, "Laser time-of-flight mass spectrometry for space," *Review of Scientific Instruments*, vol. 71, no. 2 I, pp. 536–545, 2000.

[18] G. G. Managadze and I. Y. Shutyaev, *Chemical Analysis*, vol. 124, John Wiley & Sons, New York, NY, USA, 1993.

[19] L. M. Zelenyi and A. V. Zakharov, "Phobos-grunt project: devices for scientific studies," *Solar System Research*, vol. 44, no. 5, pp. 359–361, 2010.

[20] G. G. Managadze, P. Wurz, R. Z. Sagdeev et al., "Study of the main geochemical characteristics of phobos' regolith using laser time-of-flight mass spectrometry," *Solar System Research*, vol. 44, no. 5, pp. 376–384, 2010.

[21] Y. Lin, Q. Yu, W. Hang, and B. Huang, "Progress of laser ionization mass spectrometry for elemental analysis—a review of the past decade," *Spectrochimica Acta B*, vol. 65, no. 11, pp. 871–883, 2010.

[22] Q. Yu, L. Chen, R. Huang et al., "Laser ionization time-of-flight mass spectrometry for direct elemental analysis," *Trends in Analytical Chemistry*, vol. 28, no. 10, pp. 1174–1185, 2009.

[23] R. E. Honig and J. R. Woolston, "Laser-induced emission of electrons, ions, and neutral atoms from solid surfaces," *Applied Physics Letters*, vol. 2, no. 7, pp. 138–139, 1963.

[24] N. C. Fenner, "Ion energies in the plasma produced by a high power laser," *Physics Letters*, vol. 22, no. 4, pp. 421–422, 1966.

[25] M. Southon, M. Witt, A. Harris, E. Wallach, and J. Myatt, "Laser-microprobe mass-analysis of surface layers and bulk solids," *Vacuum*, vol. 34, no. 10-11, pp. 903–909, 1984.

[26] J. He, R. Huang, Q. Yu, Y. Lin, W. Hang, and B. Huang, "A small high-irradiance laser ionization time-of-flight mass spectrometer," *Journal of Mass Spectrometry*, vol. 44, no. 5, pp. 780–785, 2009.

[27] M. Tulej, M. Iakovleva, I. Leya, and P. Wurz, "A miniature mass analyser for in-situ elemental analysis of planetary material-performance studies," *Analytical and Bioanalytical Chemistry*, vol. 399, no. 6, pp. 2185–2200, 2011.

[28] S. Scherer, K. Altwegg, H. Balsiger et al., "A novel principle for an ion mirror design in time-of-flight mass spectrometry," *International Journal of Mass Spectrometry*, vol. 251, no. 1, pp. 73–81, 2006.

[29] X. Wang, S. Amoruso, A. Tortora et al., "Analysis of charged fragments emitted during excimer laser ablation of YNi2B2C borocarbide targets by time-of-flight mass spectrometry," *Applied Surface Science*, vol. 186, no. 1–4, pp. 303–308, 2002.

[30] L. Torrisi, "Fractional ionization in plasmas produced by pulsed laser ablation," *Radiation Effects and Defects in Solids*, vol. 157, no. 3, pp. 347–356, 2002.

[31] L. Torrisi, G. Ciavola, S. Gammino et al., "Metallic etching by high power Nd:yttrium-aluminum-garnet pulsed laser irradiation," *Review of Scientific Instruments*, vol. 71, no. 11, pp. 4330–4334, 2000.

[32] A. Riedo, P. Wahlström, J. A. Scheer, P. Wurz, and M. Tulej, "Effect of long duration UV irradiation on diamondlike carbon surfaces in the presence of a hydrocarbon gaseous atmosphere," *Journal of Applied Physics*, vol. 108, no. 114915, 2010.

[33] S. Amoruso, A. Amodeo, V. Berardi, R. Bruzzese, N. Spinelli, and R. Velotta, "Laser produced plasmas in high fluence ablation of metallic surfaces probed by time-of-flight mass spectrometry," *Applied Surface Science*, vol. 96–98, pp. 175–180, 1996.

[34] J. Álvarez-Ruiz, M. López-Arias, R. De Nalda, M. Martín, A. Arregui, and L. Bañares, "Generation of CdS clusters using laser ablation: the role of wavelength and fluence," *Applied Physics A*, vol. 95, no. 3, pp. 681–687, 2009.

[35] V. Ignatova, L. Van Vaeck, R. Gijbels, and F. Adams, "Molecular speciation of inorganic mixtures by Fourier transform laser microprobe mass spectrometry," *International Journal of Mass Spectrometry*, vol. 225, no. 3, pp. 213–224, 2003.

[36] B. Yan, L. Li, Q. Yu, W. Hang, J. He, and B. Huang, "High irradiance laser ionization mass spectrometry for direct speciation of iron oxides," *Journal of the American Society for Mass Spectrometry*, vol. 21, no. 7, pp. 1227–1234, 2010.

[37] R. Torres and M. Martin, "Laser ablation and time-of-flight mass-spectrometric study of SiO," *Applied Surface Science*, vol. 193, no. 1–4, pp. 149–155, 2002.

[38] R. Hergenröder, O. Samek, and V. Hommes, "Femtosecond laser ablation elemental mass spectrometry," *Mass Spectrometry Reviews*, vol. 25, no. 4, pp. 551–572, 2006.

[39] R. K. Boyd, C. Basic, and R. A. Bethem, *Trace Quantitative Analysis by Mass Spectrometry*, John Wiley & Sons, 2008.

[40] H. Y. McSween Jr. and G. R. Huss, *Cosmochemistry*, Cambridge University Press, Cambridge, UK, 2010.

[41] F. Aubriet, C. Poleunis, J. F. Muller, and P. Bertrand, "Laser ablation and secondary ion mass spectrometry of inorganic transition-metal compounds. Part I: comparison between static ToF-SIMS and LA-FTICRMS," *Journal of Mass Spectrometry*, vol. 41, no. 4, pp. 527–542, 2006.

[42] L. Van Vaeck, A. Adriaens, and F. Adams, "Microscopical speciation analysis with laser microprobe mass spectrometry and static secondary ion mass spectrometry," *Spectrochimica Acta B*, vol. 53, no. 2, pp. 367–378, 1998.

[43] B. Maunit, A. Hachimi, P. Manuelli, P. J. Calba, and J. F. Muller, "Formation of iron oxides clusters induced by

resonant laser ablation/ionization," *International Journal of Mass Spectrometry and Ion Processes*, vol. 156, no. 3, pp. 173–187, 1996.

[44] A. T. De Ville D'Avray, E. E. Carpenter, C. J. O'Connor, and R. B. Cole, "Characterization of ferrite nanoparticles by laser desorption/ionization mass spectrometry," *European Journal of Mass Spectrometry*, vol. 4, no. 6, pp. 441–449, 1998.

[45] F. Aubriet and J. F. Muller, "About the atypical behavior of CrO_3, MoO_3, and WO_3 during their UV laser ablation/ionization," *Journal of Physical Chemistry A*, vol. 106, no. 25, pp. 6053–6059, 2002.